2005 American Control Conference
June 8-10, 2005. Portland, OR, USA

Fundamental Spatial Performance Limitation Analysis of Multiple Array Paper Machine Cross-directional Processes

Junqiang Fan and Gregory E. Stewart

***Abstract*— This paper presents a fundamental spatial performance limitation analysis method for multiple array paper machine cross-directional (CD) processes based on a two-dimensional (temporal and spatial) frequency decomposition method. Paper machine CD processes are spatially-distributed dynamical systems. Due to their (almost) spatially invariant characteristic, the models of these systems are considered as transfer matrices with rectangular circulant matrix blocks, whose input and output singular vectors are the Fourier components of dimension equivalent to number of actuators and measurements respectively. Through this method, a fundamental spatial performance limitation of multiple array CD processes can be observed. A real industrial multiple array CD process is used for illustrating the effectiveness of this method.**

I. INTRODUCTION

This paper is motivated by an industrial multiple array paper machine cross-directional (CD) process control problem. A typical multiple array paper machine CD process usually includes $1 \sim 7$ actuator arrays (each array has tens to hundreds of spatially distributed actuators) and $3 \sim 5$ controlled sheet properties (each property has hundreds to thousands of spatially distributed measurements). Before any controller design, we may want to find out how difficult the plant is to control and what are the performance limitations. That is, we want to follow the guidelines of input-output controllability analysis proposed in [1] and analyze spatial performance limitation for multiple array CD processes.

An industrial paper machine is shown in Fig. 1 which is installed with CD actuator arrays, such as slice lip, steam box, rewet shower, and induction heating actuators. The scanning sensors are used for measuring the paper sheet properties, such as dry weight, moisture, and caliper. The control objective is to keep the variability of these properties as small as possible by adjusting the CD actuator arrays.

It is known that one actuator array may affect more than one controlled property [2]–[6]. For example, the slice lip actuators illustrated in Fig. 1 although designed to control the dry weight profile only, can have an impact on the dry weight, moisture and caliper profiles. Fig. 2 shows the steady-state responses of dry weight and moisture to slice lip actuators on a linerboard paper machine in the USA. Figs. 2a and b show the dry weight and moisture profiles

This work was supported by Honeywell, the Natural Sciences and Engineering Research Council of Canada, and Technology Partnerships Canada.

J. Fan and G.E. Stewart are with Honeywell Automation and Control Solutions, 500 Brooksbank Ave, North Vancouver, BC, Canada, V7J 3S4. {james.fan,greg.stewart}@honeywell.com

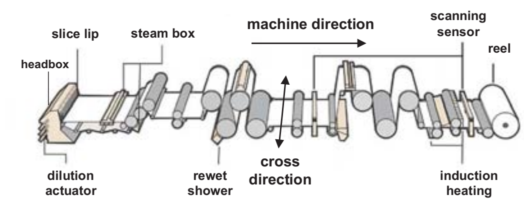

Fig. 1. Wide view of the paper machine showing typical positions of the various actuator arrays and scanning sensor(s).

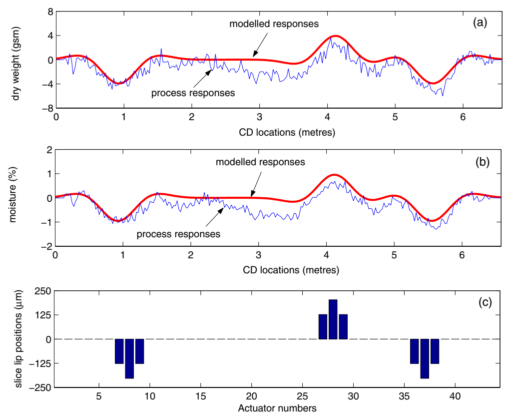

Fig. 2. (a) Steady-state response of dry weight due to moving slice lip actuators as shown in (c); (b) Response of moisture profile; (c) The slice lip actuator profile. Data was obtained from a linerboard paper machine in the USA.

including the process responses and the modelled responses respectively, and Fig. 2c shows the actuator profile. Note that all of these figures are showing the deviations attributed to the bump test. Field personnel typically use pairing rules to choose one actuator array for controlling one paper property and the interaction of multiple array CD processes has traditionally been neglected in CD control. For example, slice lip is paired to dry weight and steam box is paired to moisture even though slice lip affects both dry weight and moisture. However, with development of modern technologies, such as computer hardware and control algorithms, it is possible to optimally control several paper properties using multiple actuator arrays [6], [7]. Significant performance improvement and energy consumption reduction by using this multiple array controller has been reported in [6], [7] compared to a traditional single array controller.

The majority of the literature for CD process identification and control are related to single actuator array and single sheet property cases. The spatial frequency analysis

0-7803-9098-9/05/$25.00 ©2005 AACC

and spatial bandwidth of single array CD systems have been well addressed in [8], [9]. CD controller designs based on singular value decomposition (SVD) method have been proposed in [10]–[15]. The ill-conditioning feature is common in most single array CD process model matrices [16]–[18] because the smallest singular value of these model matrices is typically close to zero and potentially as many as a third of singular values are close to zero even at steady-state. Performance limitation for single array CD processes due to uncertain signs of the small modal gains may be found in [13]. Recently, a method based on rectangular circulant matrices has been proposed for analyzing CD process control [19], [20] in the two-dimensional (temporal and spatial) frequency domain. Analysis of steady-state performance for single array CD control is also addressed in [21] as steady-state performance is one of most important performance indices for CD control. The practical problems imposed by multiple array CD processes have begun to be treated in the industrial literature [2], [4], [5], [7], [22].

This paper analyzes multiple array CD processes in the two-dimensional frequency domain [19], [20]. The huge transfer function matrix (the process model) is composed of near-rectangular circulant matrix (RCM) blocks and can be transformed into a sequence of small dimension transfer function matrices across the spatial frequency domain by pre- and post- multiplication of Fourier matrices [23] and permutation matrices [1]. Then all of the singular values of the process model can be obtained through using singular value decomposition (SVD) for these small dimension transfer function matrices across the spatial frequencies. Therefore, spatial performance limitations of a multiple array CD process can be directly linked to the singular values in the spatial frequency domain. The main contributions of this paper are: (1) providing an intuitive and practical spatial performance limitation analysis method for multiple array CD processes; (2) illustrating that the ill-conditioning of multiple array CD process could be due to multivariable interaction between actuator and measurement arrays as well as the ill-conditioning due to low gain at high spatial frequencies familiar from single array processes.

II. Multiple Array CD Process Model

In this paper, a real linerboard paper machine in the USA is used as a typical multiple array CD process example. This paper machine has two headboxes - primary and secondary - each outfitted with its respective slice lip actuator array. The machine is further instrumented with one rewet shower actuator array such that the total number of actuator arrays $N_u = 3$. Both of the slice lip actuator arrays (u_1 and u_2) have $n_1 = n_2 = 44$ actuators and the rewet shower actuator array (u_3) has $n_3 = 88$ actuators[1]. The controlled sheet properties are dry weight and moisture (the number of measurement arrays $N_y = 2$) which are measured by the same scanner and have the same resolution, i.e., the number of measurements is $m = 264$ after scanner signal processing. Here are the multiple array CD process model $\mathbf{G}(z)$ and a controller $K(z)$,

$$\begin{aligned} Y(z) &= \mathbf{G}(z)U(z) + D(z), && (1)\\ \mathbf{G}(z) &= \begin{bmatrix} G_{11}(z) & G_{12}(z) & 0 \\ G_{21}(z) & G_{22}(z) & G_{23}(z) \end{bmatrix}, && (2)\\ G_{ij}(z) &= B_{ij} \cdot h_{ij}(z), && (3)\\ U(z) &= K(z)Y(z), && (4) \end{aligned}$$

where

$$\begin{aligned} Y(z) &= \left[y_1(z)^T, y_2(z)^T\right]^T \in \mathbb{C}^{528\times 1},\ y_i(z) \in \mathbb{C}^{264\times 1},\\ U(z) &= \left[u_1(z)^T, u_2(z)^T, u_3(z)^T\right]^T \in \mathbb{C}^{176\times 1},\\ & \quad\ u_1(z),\ u_2(z) \in \mathbb{C}^{44\times 1},\ u_3(z) \in \mathbb{C}^{88\times 1},\\ D(z) &= \left[d_1(z)^T, d_2(z)^T\right]^T \in \mathbb{C}^{528\times 1},\ d_i(z) \in \mathbb{C}^{264\times 1},\\ h_{ij}(z) &= \frac{z^{-p_{ij}}}{1 - a_{ij}z^{-1}},\ \ i = 1,2,\ \ j = 1,2,3,\\ K(z) &\in \mathbb{C}^{176\times 528}, \end{aligned}$$

where $Y(z)$, $U(z)$ and $D(z)$ are the $\mathscr{Z}$-transforms of the measurement profile (y_1: dry weight, and y_2: moisture), the actuator profile (u_1: primary slice lip, u_2: secondary slice lip, and u_3: rewet shower), and the disturbance profile (d_1: dry weight disturbance, and d_2: moisture disturbance) respectively; B_{ij} is the $(i, j)^{\text{th}}$ interaction matrix which describes the spatial response of the $(i, j)^{\text{th}}$ process; $h_{ij}(z)$ is the $\mathscr{Z}$-transform of the temporal response of the $(i, j)^{\text{th}}$ process, the integer p_{ij} represents the $(i, j)^{\text{th}}$ process dead time, and a_{ij} is related to the $(i, j)^{\text{th}}$ process time constant and the sampling time. Note that the rewet shower actuator array has no impact on the dry weight as expected.

The spatial interaction matrices B_{ij} and the temporal response $h_{ij}(z)$ are identified from input-output data by an industrial software tool [22]. Like most other published CD models, in this work, each actuator within an array is considered to have the same spatial response shape. That is, spatial invariance is assumed to be held for the spatial interaction matrices B_{ij} except edges, where the spatial responses are truncated [24]. This assumption is based on models identified from hundreds of real paper machines. The spatial interaction matrices B_{ij} in (3) are usually ill-conditioned such that $\frac{\overline{\sigma}(B_{ij})}{\underline{\sigma}(B_{ij})} \gg 1$ as discussed in [9], [13], [14], [16], [17].

We assume the multiple array CD process model $\mathbf{G}(z)$ in (1) has been properly scaled. A detailed description of scaling of multi-array systems is omitted for brevity. In practice, a technique based on the scaling method in [25] modified for spatially distributed systems is used.

For single array CD processes, the spatial bandwidth may be computed from single actuator's spatial response [9]. It is known that smaller singular values of a single array CD process model are typically related to high spatial frequencies while its larger singular values correspond to lower

[1]Note it is a coincidence to find the numbers of actuator arrays related by integer ratio as we find here. Generally no such relationship may be assumed, and our work does not depend on this restricted form.

spatial frequencies [8], [18], [20]. Typically, for a single CD array process, lower spatial frequency disturbances are controllable while higher spatial frequency ones are difficult to control or not controllable at all, which is very familiar in industrial CD control. However, the question is, for a given multiple array CD process, whether it is possible to provide papermakers with practical insight into the level of performance that may be achieved without requiring to perform a full controller design. Is it true that any combinations of disturbances (i.e., different directions) are controllable at lower spatial frequency range for a multiple array CD process?

In the following two sections, a method based on rectangular circulant matrices [20] is used for analyzing multiple array CD processes and the singular values of the process model $\mathbf{G}(z)$ in (1) can be sorted through spatial frequencies.

III. Temporal and Spatial Frequencies

This section is an overview of rectangular circulant matrices (RCMs) and the relationship between the singular values of single array systems and the spatial frequencies presented in [19], [20], [26].

The RCM is defined as:

Definition 1: A matrix $R \in \mathbb{C}^{m\times n}$ is a rectangular circulant matrix if it satisfies the following conditions:

1) *If $m = n_a \cdot n$, then column j = column $j-1$ circularly down shifted n_a times, $j = 2,3,\cdots,n$,*
2) *If $n = n_a \cdot m$, then row k=row $k-1$ circularly right shifted n_a times, $k = 2,3,\cdots,m$,*

for a positive integer n_a.

Strictly speaking, the single array CD models (such as $G_{ij}(z)$ in (2)) are not exact RCMs due to non-periodic boundary conditions imposed by the paper sheet edges and non-integer multiple relationship between the dimensions of the actuator array and the measurements. However, these effects are typically minor in practice [20]. Therefore, in this article, the single array models $G_{ij}(z)$ and the multiple array model $\mathbf{G}(z)$ in (2) are approximated as RCMs and RCM blocks, which are denoted as the following symbols,

$$\overline{\mathbf{G}}(z) = \begin{bmatrix} \overline{G}_{11}(z) & \overline{G}_{12}(z) & 0 \\ \overline{G}_{21}(z) & \overline{G}_{22}(z) & \overline{G}_{23}(z) \end{bmatrix}. \qquad (5)$$

It is known that these single CD arrays systems $\overline{G}_{ij}(z)$ are spatial frequency bandlimited[2] [9]. For the majority of CD processes, this frequency $\nu_{B_{ij}}$ is smaller than the spatial Nyquist frequency at the actuator resolution, which is defined by

$$\nu_{B_{ij}} < \nu_N^{u_j} = \frac{1}{2d_{u_j}}, \qquad (6)$$

where d_{u_j} is the j^{th} actuator spacing. Therefore, $\overline{G}_{ij}(z)$ in (5) are spatial frequency bandlimited RCMs [20].

[2]There exists a spatial frequency $\nu_{B_{ij}}$ such that the magnitudes of the frequency components of all columns of B_{ij} in (3) above $\nu_{B_{ij}}$ are zeros [20].

Two important properties of a spatial frequency bandlimited RCM $R(z) \in \mathbb{C}^{m\times n}$ are that their two-dimensional frequency representations and their singular values can be obtained as follows,

$$\{r(\nu_1^u, z), \cdots, r(\nu_n^u, z)\} = \mathbf{DIAG}(F_m R(z) F_n^H), \qquad (7)$$
$$\sigma_j(R(z)) = \left| r(\nu_j^u, z) \right|, \quad j = 1,\cdots,n, \qquad (8)$$

where $F_m \in \mathbb{C}^{m\times m}$ and $F_n \in \mathbb{C}^{n\times n}$ are the complex Fourier matrices, H denotes the conjugate transpose, $r(\nu_j^u, z)$ are the representations of $R(z)$ in the two-dimensional frequency domain and they are SISO transfer functions for the discrete spatial frequencies ν_j. The operation '$\mathbf{DIAG}(X)$' with a rectangular matrix $X \in \mathbf{C}^{m\times n}$ is to get the following elements of X into a vector,

$$\mathbf{DIAG}(X) = \{X(1,1), \cdots, X(k,k), X((n_a-1)n+k+1, k+1), \cdots, X(m,n)\}, \qquad (9)$$

where $k = n/2$ for even n or $k = (n+1)/2$ for odd n (straightforward extension for the case $X \in \mathbb{C}^{n\times m}$).

Let $\widetilde{G}_{ij}(z)(= F_m \overline{G}_{ij}(z) F_{n_j}^H)$ represent the model in the spatial frequency domain, where $m = 264, n_j = 44$ or 88. Note that $\widetilde{G}_{ij} \in \mathbb{C}^{m\times n_j}$ has the diagonal nonzero elements as illustrated in Fig. 3, which represent spatial frequency gains, due to its RCM characteristic [20].

In Fig. 3, $g_{ij}(\nu_0, z)$ is the gain at zero spatial frequency, $g_{ij}(\nu_1, z)$ and $\widetilde{g}_{ij}(\nu_1, z)$ are conjugate and represent the same spatial frequency gain with different phases, $p = q-1 = 21$ for $n_j = 44$, and $p = q-1 = 43$ for $n_j = 88$, where n_j is the number of columns of $\widetilde{G}_{ij}$ (i.e., the numbers of actuator arrays).

IV. Fundamental Spatial Performance Limitation Analysis for Multiple Array CD Processes

In this section, we will present the framework for analyzing the multiple array CD processes in terms of spatial and temporal frequencies. Connections to the singular value decomposition are made.

A. The multiple array CD process model in the two-dimensional frequency domain

First, two large Fourier matrices are constructed for the multiple sheet measurements $Y(z)$ and the multiple actuator

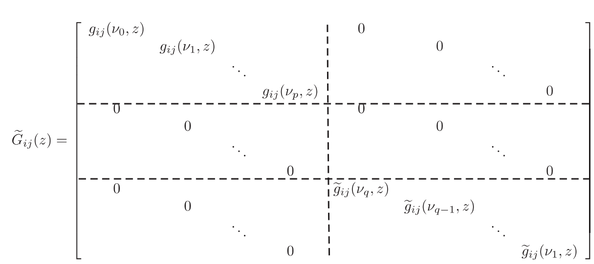

Fig. 3. Diagonal property of the subplant model $G_{ij}(z)$ in the spatial frequency domain.

arrays $U(z)$ respectively,

$$\mathbf{F}_y = diag(F_m, F_m) \in \mathbb{C}^{528\times528}, \quad (10)$$
$$\mathbf{F}_u = diag(F_{n_1}, F_{n_2}, F_{n_3}) \in \mathbb{C}^{176\times176}, \quad (11)$$

where $F_m \in \mathbb{C}^{264\times264}$ and $F_{n_j} \in \mathbb{C}^{n_j\times n_j}$ with $n_1 = 44$, $n_2 = 44$, and $n_3 = 88$ are the complex Fourier matrices for the i^{th} controlled property and the j^{th} actuator array respectively. Then, the multiple array CD process model in the two-dimensional frequency domain can be obtained through

$$\widetilde{\mathbf{G}}(z) = \mathbf{F}_y \overline{\mathbf{G}}(z) \mathbf{F}_u^H \quad (12)$$
$$= \begin{bmatrix} \widetilde{G}_{11}(z) & \widetilde{G}_{12}(z) & 0 \\ \widetilde{G}_{21}(z) & \widetilde{G}_{22}(z) & \widetilde{G}_{23}(z) \end{bmatrix} \quad (13)$$

where each

$$\widetilde{G}_{ij}(z) = F_m \overline{G}_{ij}(z) F_{n_j}^H. \quad (14)$$

Note that due to different actuator numbers among the actuator arrays (i.e., different spatial Nyquist frequencies ν_N^u), $\widetilde{G}_{ij}(z)$ may not appear in (13) for some spatial frequencies. For example, for the given plant, the actuator spacings for the primary slice lip, secondary slice lip, and rewet shower actuators are $d_u = 0.15, 0.15$, and 0.075 metres, respectively. If the spatial frequency $\nu > \nu_N^{u_1} = \frac{1}{2d_u} = 3.33$ cycles/metre, the matrices $\widetilde{G}_{11}(z)$, $\widetilde{G}_{12}(z)$, $\widetilde{G}_{21}(z)$, and $\widetilde{G}_{22}(z)$ do not appear in (13) due to the fact that the Nyquist frequencies $\nu_N^{u_1} = 3.33$ cycles/metre for the slice lips and $\nu_N^{u_2} = 6.67$ cycles/metre for the rewet shower actuators, then only the rewet shower actuation is available at spatial frequencies $3.33 < \nu < 6.67$ cycles/metre.

Fig. 4 illustrates the scaled steady-state spatial frequency responses of each subplant $\overline{G}_{ij}(z)|_{z=1}$ in (5).

B. Singular values in the spatial frequency domain

Pre- and post-multiplication of unitary matrices to a matrix will not change its singular values [1]. The Fourier matrices $\mathbf{F}_y$ in (10) and $\mathbf{F}_u$ in (11) are unitary matrices

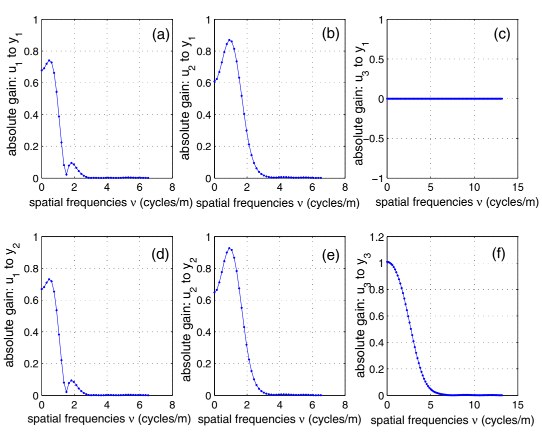

Fig. 4. Scaled steady-state spatial frequency responses of the multiple array CD process model $\overline{\mathbf{G}}(z)$ in (5).

$$\widehat{\mathbf{G}}(z) = \left[\begin{array}{ccccccc} g(\nu_0,z) &&&&&& \\ & g(\nu_1,z) &&&&& \\ && \widetilde{g}(\nu_1,z) &&&& \\ &&& \ddots &&& \\ &&&& g(\nu_k,z) && \\ &&&&& \widetilde{g}(\nu_k,z) & \\ &&&&&& \ddots \\ \hdashline 0 &&& \cdots &&& 0 \\ \vdots &&& \ddots &&& \vdots \\ 0 &&& \cdots &&& 0 \end{array}\right] \quad \widehat{\mathbf{G}}_1(z)$$

Fig. 5. Block diagonal property of $\widehat{\mathbf{G}}(z)$ after unitary permutation of $\widetilde{\mathbf{G}}(z)$.

[23], therefore, $\overline{\mathbf{G}}(z)$ in (5) and $\widetilde{\mathbf{G}}(z)$ in (12) have the same singular values.

It is always possible to find two (unitary) permutation matrices[3] P_y and P_u for transforming $\widetilde{\mathbf{G}}(z)$ in (12) into a block-diagonal matrix $\widehat{\mathbf{G}}(z)$ [11],

$$\widehat{\mathbf{G}}(z) = P_y \widetilde{\mathbf{G}}(z) P_u, \quad (15)$$

where $P_y \in \mathbb{R}^{528\times528}$ and $P_u \in \mathbb{R}^{176\times176}$. The matrix $\widehat{\mathbf{G}}(z)$ is illustrated in Fig. 5, where $g(\nu_0,z)$, $g(\nu_k,z)$, and $\widetilde{g}(\nu_k,z)$ are obtained through (due to limited space in the following 3 equations, we will suppress the argument (ν_k,z) in $g_{ij}(\nu_k,z)$ and $\widetilde{g}_{ij}(\nu_k,z)$)

$$g(\nu_0,z) = \begin{bmatrix} g_{11} & g_{12} & 0 \\ g_{21} & g_{22} & g_{23} \end{bmatrix}, \quad (16)$$

$$g(\nu_k,z) = \begin{cases} \begin{bmatrix} g_{11} & g_{12} & 0 \\ g_{21} & g_{22} & g_{23} \end{bmatrix}, & \text{for } k = 1, \cdots, 22, \\ \begin{bmatrix} 0 \\ g_{23} \end{bmatrix}, & \text{for } k = 23, \cdots, 44, \end{cases} \quad (17)$$

$$\widetilde{g}(\nu_k,z) = \begin{cases} \begin{bmatrix} \widetilde{g}_{11} & \widetilde{g}_{12} & 0 \\ \widetilde{g}_{21} & \widetilde{g}_{22} & \widetilde{g}_{23} \end{bmatrix}, & \text{for } k = 1, \cdots, 22, \\ \begin{bmatrix} 0 \\ \widetilde{g}_{23} \end{bmatrix}, & \text{for } k = 23, \cdots, 44, \end{cases} \quad (18)$$

where g_{ij} in (16) denotes $g_{ij}(\nu_0,z)$, g_{ij} in (17) and $\widetilde{g}_{ij}$ in (18) represent $g_{ij}(\nu_k,z)$ and $\widetilde{g}_{ij}(\nu_k,z)$ respectively, $\nu_k = 0.1515 \cdot k$ cycles/metre. As mentioned above, $g_{ij}(\nu_k,z)$ and $\widetilde{g}_{ij}(\nu_k,z)$ have the same spatial frequency gain with different phases.

Since $\widehat{\mathbf{G}}(z) \in \mathbb{C}^{528\times176}$ has the same singular values as the nonzero block-diagonal matrix $\widehat{\mathbf{G}}_1(z) \in \mathbb{C}^{176\times176}$ in Fig. 5, then the singular values of $\widehat{\mathbf{G}}_1(z)$ can be obtained through solving the singular values of the small matrices $g(\nu_0,z)$, $g(\nu_k,z)$, and $\widetilde{g}(\nu_k,z)$ which are sorted through spatial frequencies from low to high. Finally we can obtain the singular values of $\overline{\mathbf{G}}(z)$ in (5) according to spatial frequencies. That is, if $\overline{\mathbf{G}}(z)$ is composed of spatial frequency bandlimited RCM [20] blocks as mentioned in Section III,

[3]A permutation matrix has a single 1 in every row and column and all other elements equal to 0 [1].

and let

$$
\begin{aligned}
s_1^T \quad &:= \quad [\Sigma(g(\nu_0,z)),\Sigma(g(\nu_1,z)),\Sigma(\widetilde{g}(\nu_1,z)), \\
&\qquad \cdots,\Sigma(g(\nu_{44},z)),\Sigma(\widetilde{g}(\nu_{44},z))], \qquad (19)\\
s_2^T \quad &:= \quad [\sigma_1(\overline{\mathbf{G}}(z)),\sigma_2(\overline{\mathbf{G}}(z)),\cdots,\sigma_{176}(\overline{\mathbf{G}}(z))], \quad (20)
\end{aligned}
$$

where s_1 and s_2 are column vectors of singular values, and $\Sigma(A)$ is defined as

$$\Sigma(A) \quad = \quad [\overline{\sigma}(A),\cdots,\underline{\sigma}(A)], \tag{21}$$

then,

$$s_1 = P\cdot s_2, \tag{22}$$

where $P\in\mathbb{R}^{176\times176}$ is a permutation matrix.

Note that in s_2 of (20), the singular values of $\overline{\mathbf{G}}(z)$ are sorted through their magnitudes. Therefore, there is no link between these singular values and spatial frequencies. Most multiple array CD process models $\overline{\mathbf{G}}(z)$ are ill-conditioned even at steady-state ($\omega = 0$), and it is difficult to intuitively interpret which spatial frequency range are controllable and which are not controllable through an SVD analysis alone. However, through s_1 of (19), all the singular values are sorted through the spatial frequencies, and it is straightforward to analyze the process in terms of the individual transfer matrices $g(\nu_k,z)\in\mathbb{C}^{2\times3}$ for $k = 1,\cdots,22$ or $g(\nu_k,z)\in\mathbb{C}^{2\times1}$ for $k = 23,\cdots,44$. Further, the spatial performance limitations of the plant can be analyzed through spatial frequencies, which will be explored in the next subsection.

C. Spatial performance limitation analysis

From a practical point of view, due to inevitable model uncertainty and possible physical limits on the actuator arrays, the disturbances aligned with the weak singular vector directions, which correspond to the smaller singular values, are difficult to be rejected by a feedback controller. Some multiple array CD process models are ill-conditioned at very low spatial and temporal frequencies due to interaction between multiple actuator and measurement arrays (i.e., $\overline{\sigma}(g(\nu_k,z))/\underline{\sigma}(g(\nu_k,z)) \gg 1$ for $\nu_k\approx0,\ \omega\approx0$), for example, the supercalendar process described in [7]. That means some disturbance directions are not controllable even at very low spatial and temporal frequencies. Low spatial frequency disturbances are typically considered to be controllable for single CD array systems, because there is no directionality problem, which can exist in some multiple array CD processes. Due to the length limit of the paper, we will not present a real multiple array CD process model which is ill-conditioned at very low spatial frequencies (the reader is referred to [7], [27]).

For CD processes, the controllable capability of the closed-loop systems at steady-state ($z = 1$) is important to papermakers. It is usually required that the steady-state disturbances be rejected as much as possible. Fig. 6 shows the singular values of the multiple array nominal CD

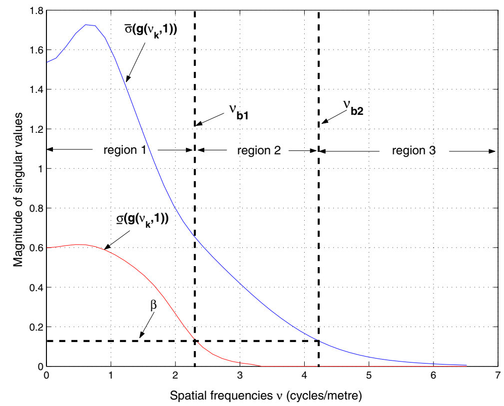

Fig. 6. Singular values of the steady-state process model across the spatial frequencies.

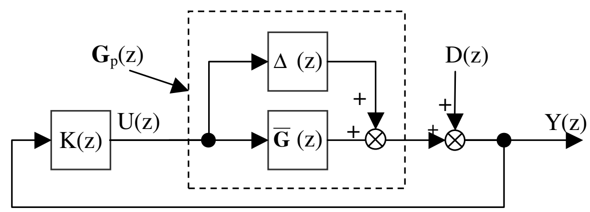

Fig. 7. A feedback closed-loop system diagram.

process model $\overline{\mathbf{G}}(z)$ in (5) at steady-state ($z = 1$) according to spatial frequencies.

The uncertainty in the plant as shown in Fig. 7 is modelled in terms of a linear stable unstructured matrix perturbation,

$$
\begin{aligned}
\mathbf{G}_p(z) \quad &:= \quad \overline{\mathbf{G}}(z)+\Delta(z), &(23)\\
\overline{\sigma}(\Delta(e^{j\omega})) \quad &\leq \quad \beta. &(24)
\end{aligned}
$$

Note that while the nominal model $\overline{\mathbf{G}}(z)$ in (5) has an RCM structure, the perturbed plant $\mathbf{G}_p(z)$ does *not* necessarily have an RCM structure due to the presence of the unstructured matrix $\Delta(z)$.

For the additive unstructured model uncertainty $\Delta(z)$ in (23) (also shown in Fig. 7), the robust stability (RS) condition is given by the small gain theorem [1], here

$$\overline{\sigma}(M(e^{j\omega})\Delta(e^{j\omega})) \leq \overline{\sigma}(M(e^{j\omega}))\overline{\sigma}(\Delta(e^{j\omega})) < 1, \forall\omega, \tag{25}$$

where $M(z)$ and $\Delta(z)$ are assumed to be stable, and $M(z)$ ($z = e^{j\omega}$) is the closed-loop transfer function between $D(z)$ and $U(z)$ from (1) and (4),

$$M(z) = K(z)(I-\overline{\mathbf{G}}(z)K(z))^{-1}. \tag{26}$$

It is useful to rewrite the robust stability condition (25) in terms of the actuator signal,

$$\overline{\sigma}(M(e^{j\omega})) = \max_{D(e^{j\omega})\neq0}\frac{||U(e^{j\omega})||_2}{||D(e^{j\omega})||_2} < \frac{1}{\beta}, \forall\omega \tag{27}$$

To gain insight into the performance limitations for the plant $\overline{\mathbf{G}}(z)$ we consider perfect steady-state nominal performance (PSSNP) which is defined as

$$Y(z) = \overline{\mathbf{G}}(z)U(z) + D(z) = 0, \quad \text{for } z = 1. \tag{28}$$

The definition PSSNP in (28) is similar as perfect control defined in [1], which is used for performance limitation analysis.

However, the matrix $\overline{\mathbf{G}}(z)$ in (5) is composed of submatrices $\overline{G}_{ij}(z)$ each of whom are typically rank-deficient. The rank-deficiency is due to the measurements outnumbering the actuators and also the spatially distributed nature of the plant model [8], [13], [16].

Then the best control possible is achieved with PSSNP on the components of $Y(z)$ which align with singular vectors that correspond to nonzero singular values of the plant $\overline{\mathbf{G}}(z)$. Imposing this condition leads to a non-unique solution for $U(z)|_{z=1}$ in (28). In order to best satisfy the robust stability condition (27) the specific solution that minimizes the actuator effort $||U(1)||_2$ is given by,

$$U(z) = -\overline{\mathbf{G}}^{\dagger}(z)D(z), \quad \text{for } z = 1, \tag{29}$$

where $\overline{\mathbf{G}}^{\dagger}(z)$ denotes the pseudo-inverse of $\overline{\mathbf{G}}(z)$.

The following theorem presents a practical result to classify the components of $Y(z)$ in (28) which may be perfectly controlled without violating the robust stability condition.

Theorem 1: For a multiple array CD process, if each subplant $\overline{G}_{ij}(z)|_{z=1}$ in (5) is an RCM and its spatial frequency bandwidth satisfies $\nu_{B_{ij}} \leq \nu_N^{u_j}$ in (6), and the maximum singular value of the unstructured model uncertainty $\overline{\sigma}(\Delta(z)|_{z=1}) \leq \beta$ in (24), there exists a controller $K(z)$ in (4) that satisfies (i) PSSNP at spatial frequency $\nu = \nu_k$; (ii) robust stability in (25) only if the process model gain satisfies

$$\underline{\sigma}(g(\nu_k, z)|_{z=1}) > \beta, \tag{30}$$

at spatial frequency $\nu = \nu_k$.

Proof: At steady-state, the nominal perfect control requires $M(1) = -\overline{\mathbf{G}}^{\dagger}(1)$. Then $\overline{\sigma}(M(1)) = \overline{\sigma}(\overline{\mathbf{G}}^{\dagger}(1)) = 1/\underline{\sigma}(\overline{\mathbf{G}}(1))$. At steady-state, from (25), the RS condition requires $\overline{\sigma}(M(1)) = 1/\underline{\sigma}(\overline{\mathbf{G}}(1)) < 1/\overline{\sigma}(\Delta(1))$. That is, $\underline{\sigma}(\overline{\mathbf{G}}(1)) > \beta \geq \overline{\sigma}(\Delta(1))$. As $\overline{\mathbf{G}}(1)$ is a spatial frequency bandlimited RCM-block matrix, from (19) to (22), $\underline{\sigma}(g(\nu_k, 1)) > \beta$, for all ν_k. $\square$

Remark: The requirement of RCM structure for each subplant $\overline{G}_{ij}(z)|_{z=1}$ in the above theorem needs integer ratio between the number of measurements m and the number of actuator array n_j according to Definition 1. Theorem 1 can be extended to cover all practical CD systems when m/n_j is non-integer by considering the upsampling-downsampling technique in Section 4.3 of [20].

Based on the above theorem, in Fig. 6,

- In region 1 defined by the low spatial frequencies $0 \leq \nu \leq 2.3$ cycles/metre, we have $\underline{\sigma}(g(\nu_k, 1)) > \beta$. In other words, for spatial frequencies $\nu < 2.3$ cycles/metre, both the dry weight and the moisture could achieve PSSNP in (28) without necessarily violating robust stability in (24)-(25).
- In region 2 for $2.3 < \nu \leq 4.2$ cycles/metre, $\overline{\sigma}(g(\nu_k, 1)) > \beta$ but $\underline{\sigma}(g(\nu_k, 1)) < \beta$, so PSSNP of both the dry weight and the moisture would violate robust stability in (25) (note that this conclusion does *not* imply that the singular vector directions align with any physical directions).
- In region 3 for 4.2 cycles/metre $< \nu$, $\overline{\sigma}(g(\nu_k, 1)) < \beta$, so PSSNP of either the dry weight or the moisture would lead to violation of robust stability in (25).

Therefore, we can predict the best possible bandwidth (related to the maximum singular values) for this plant is ν_{b2}=4.2 cycles/metre while the worst possible bandwidth (related to the minimum singular values) is ν_{b1}=2.3 cycles/metre. It is worth noting that because there is no process gain on the dry weight after the spatial Nyquist frequencies of primary and secondary slice lip actuator arrays ν_N^u=3.33 cycles/metre, which can be verified from Figs. 4a and b. Therefore, the best possible spatial bandwidth ν_{b2} must be for the moisture profile.

V. Example

The above fundamental spatial performance limitation theorem tells what performance *cannot* be achieved for any controller but does not predict closed-loop performance will be achieved for a particular controller. In order to provide an illustrative example, a simulator was configured with a process model identified from a real USA linerboard paper machine. Its actuator and measurement profiles were initialized with their counterpart data from the machine. Here the model predictive controller in [6] is presented to illustrate typical closed-loop performance achieved with a robust controller design. Briefly stated, this controller was tuned such that $\| M(z) \|_\infty = 1/\beta$ in an effort to achieve the best nominal performance while satisfying the robust stability condition in (25).

Fig. 8 shows the data before and after control. The data before control (i.e., the steady-state disturbance $D(z)|_{z=1}$) are back-calculated by using (1) from online measurement data collected from the working paper machine[4]. The closed-loop simulator was run for 150 samples, and each sample is equivalent to one pass of the scanning sensor shown in Fig. 1. The data after control shown in Fig. 8 come from the closed-loop simulator at sample 100 (here the measurement data are considered to be at steady-state after 100 samples because there is negligible controller action after then). Figs. 8b and d show the magnitudes of the Fourier spectra of the profiles before and after control in Figs. 8a and c respectively. In Figs. 8b and d, the spatial bandwidths ν_{b1} and ν_{b2} shown in Fig. 6 are overlayed on the

[4]Calculated from D(z)=Y(z)-G(z)U(z), where Y(z) and U(z) are from real data under closed-loop control.

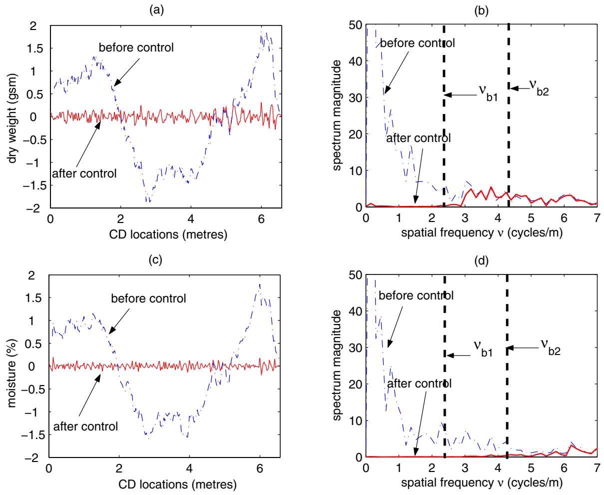

Fig. 8. (a) and (b): steady-state dry weight profiles and their spectra before and after control; (c) and (d): steady-state moisture profiles and their spectra before and after control.

closed-loop performance in order to illustrate the predictive power of the computed bandwidths in this particular case. As shown in Figs. 8b and d, PSSNP is achieved for the most part in both dry weight and moisture when the spatial frequency is smaller than ν_{b1}. PSSNP is almost achieved for moisture and not possible for dry weight when the spatial frequency is between ν_{b1} and ν_{b2}. PSSNP is not achievable for either dry weight or moisture when the spatial frequency is larger than ν_{b2}.

VI. CONCLUSIONS

This paper has presented a practical and intuitive fundamental spatial performance limitation analysis method for multiple array CD processes. The RCM-based two-dimensional frequency method has been used for transforming the multiple array CD process model. After permutation, the multiple array CD process model in the two-dimensional domain is transformed into a sequence of small dimension transfer function matrices $g(\nu_k, z)$ across the spatial frequencies. The singular values of the multiple process model can be sorted through spatial frequencies. Through investigating these singular values, we can predict the spatial performance limitation of the plant. An industrial example is illustrated through the article for verifying the effectiveness of the proposed method.

REFERENCES

[1] S. Skogestad and I. Postlethwaite, *Multivariable Feedback Control: Analysis and Design*. John Wiley & Sons, Inc., 1996.
[2] R. Hall, "Coordinated cross-machine control," in *TAPPI Proceedings of Process Control Conference*, 1989, pp. 11–19.
[3] K. Cutshall, *Paper Machine Operations, Pulp and Paper Manufacture*, 3rd ed., Atlanta and Montreal, 1991, vol. 7, ch. XVIII: Cross-direction control, pp. 472–506.
[4] J. Shakespeare, J. Pajunen, V. Nieminen, and T. Metsälä, "Robust optimal control of profiles using multiple CD actuator systems," in *Proc. Control Systems 2000*, Victoria, BC, Canada, May 2000, pp. 305–310.
[5] D. R. Saffer II, F. J. Doyle III, A. Rigopoulos, and P. Wisnewski, "MPC study for a dual headbox CD control problem," in *Proc. Control Systems 2000*, Victoria, BC, Canada, May 2000, pp. 97–100.
[6] J. U. Backström, C. Gheorghe, G. E. Stewart, and R. Vyse, "Constrained model predictive control for cross directional multi-array processes," *Pulp & Paper Canada*, vol. 102, no. 5, pp. T128–T131, May 2001.
[7] J. U. Backström, B. Henderson, and G. E. Stewart, "Identification and multivariable control of supercalenders," in *Proc. Control Systems 2002*, Stockholm, Sweden, June 2002, pp. 85–91.
[8] S. R. Duncan, "The cross-directional control of web forming process," Ph.D. dissertation, University of London, UK, 1989.
[9] S. R. Duncan and G. F. Bryant, "The spatial bandwidth of cross-directional control systems for web processes," *Automatica*, vol. 33, no. 2, pp. 139–153, February 1997.
[10] D. Laughlin, M. Morari, and R. D. Braatz, "Robust performance of cross-directional control systems for web forming processes," *Automatica*, vol. 29, no. 6, pp. 1395–1410, 1993.
[11] M. Hovd and S. Skogestad, "Control of symmetrically interconnected plants," *Automatica*, vol. 30, no. 6, pp. 957–973, 1994.
[12] M. Hovd, R. D. Braatz, and S. Skogestad, "SVD controllers for H_2-, H_∞- and μ-optimal control," *Automatica*, vol. 33, no. 3, pp. 433–439, 1997.
[13] A. P. Featherstone, J. G. VanAntwerp, and R. D. Braatz, *Identification and Control of Sheet and Film Processes*. Springer, 2000.
[14] G. E. Stewart, D. M. Gorinevsky, and G. A. Dumont, "Feedback controller design for a spatially-distributed system: The paper machine problem," *IEEE Transactions on Control Systems Technology*, vol. 11, no. 5, pp. 612–628, September 2003.
[15] O. J. Rojas, G. C. Goodwin, and G. V. Johnston, "Spatial frequency antiwindup strategy for cross-directional control problems," *Control Theory and Applications, IEE Proceedings*, vol. 149, no. 5, pp. 414–422, 2002.
[16] K. Kristinsson and G. A. Dumont, "Cross-directional control on paper machines using Gram polynomials," *Automatica*, vol. 32, no. 4, pp. 533–548, 1996.
[17] W. P. Heath, "Orthogonal functions for cross-directional control of web forming processes," *Automatica*, vol. 32, no. 2, pp. 183–198, 1996.
[18] G. E. Stewart, D. M. Gorinevsky, and G. A. Dumont, "Two-dimensional loop shaping," *Automatica*, vol. 39, no. 5, pp. 779–792, May 2003.
[19] J. Fan, "Model predictive control for multiple cross-directional processes: Analysis, tuning, and implementation," Ph.D. dissertation, The University of British Columbia, Vancouver, Canada, 2003. [Online]. Available: http://ahousat.library.ubc.ca/theses/available/etd-07142004-143355/
[20] J. Fan, G. E. Stewart, and G. A. Dumont, "Two-dimensional frequency analysis for unconstrained model predictive control of cross-directional processes," *Automatica*, vol. 40, no. 11, pp. 1891–1903, 2004.
[21] A. G. Wills and W. P. Heath, "Analysis of steady-state performance for cross-directional control," *IEE Proceedings: Control Theory Application*, vol. 149, no. 5, pp. 433–440, 2002.
[22] D. M. Gorinevsky and C. Gheorghe, "Identification tool for cross-directional processes," *IEEE Transactions on Control Systems Technology*, vol. 11, no. 5, pp. 629–640, September 2003.
[23] P. J. Davis, *Circulant Matrices (2nd Edition)*. Chelsea Publishing, 1994.
[24] S. Mijanovic, "Paper machine cross-directional control near spatial domain boundaries," Ph.D. dissertation, The University of British Columbia, Vancouver, Canada, 2004.
[25] Z. J. Lu, "Method of optimal scaling of variables in a multivariable predictive controller utilizing range control," U.S. Patent 5,574,638, Nov. 12, 1996.
[26] J. Fan, G. E. Stewart, and G. A. Dumont, "Two-dimensional frequency response analysis and insights for weight selection in cross-directional model predictive control," in *Proc. the 42nd IEEE Conference on Decision and Control*, Maui, Hawaii, USA, December 2003, pp. 3717–3723.
[27] J. U. Backström, P. He, P. Baker, and J. Fan, "Advanced multivariable CD control delivers improved quality, runnability, and profitability for different CD processes," in *Proc. Control Systems 2004*, Quebec City, Canada, June 2004.